


Characterization of the Radiation Contamination in an 18MV Linac Treatment Room Made of some Nanoparticles Mixture

Sara Ghanavati ¹, Nahid Makiabadi ¹, Sajad Keshavarz ¹, Hosein Ghiasi ^{2*} 

¹ Department of Medical Radiation Engineering, University of Science and Research Branch Tehran, Tehran, Iran

² Medical Radiation Research Team, Tabriz University of Medical Sciences, Tabriz, Iran

*Corresponding Author: Hosein Ghiasi
Email: hoseinghiasi62@gmail.com

Received: 28 March 2022/ Accepted: 27 September 2022

Abstract

Purpose: Shielding against radiation in radiotherapy and radiology requires deep knowledge of radiation physics and shielding design methods. The application of nanoparticles in the photon and neutron dose moderation has been proven in the literature.

Materials and Methods: Effective neutron mass removal cross-section (Σ_R/ρ) was for the ordinary concrete doped with 50nm in diameter nanosphers mixture of $\text{Fe}_2\text{O}_3(5\%)$, $\text{WO}_3(5\%)$, $\text{B}_4\text{H}(5\%)$, $\text{Pb}_2\text{O}_3(5\%)$ was estimated with MCNP5 Monte Carlo (MC) code and N-XCOM computational program. An 18MV linac room made of the nanoparticles dopped ordinarily simulated. Additionally, the room was considered with three legs in the maze and photoneutron and capture γ -ray Dose Equivalent (DE) were estimated at the modeled rooms maze.

Results: Total Σ_R/ρ with energies 100 keV-2000keV was estimated using MC and N-XCOM as 0.02802-0.02687 cm^2/g and 0.02810- 0.02687 cm^2/g , respectively. Total Σ_R/ρ of the neutron for the pure ordinary concrete was estimated by MC code and N-XCOM with energies 100 keV-2000keV as 0.02802-0.02687 cm^2/g and 0.02810-0.02687 cm^2/g . Borated Polyethylene (BPE) and Lead required thickness calculated as 7.43×10^{-06} mm and 4.73×10^{-06} mm for the capture γ -ray shielding.

Keywords: Monte Carlo; Neutron; N-XCOM; Dose Equivalent; Capture γ -Ray.

1. Introduction

Adequate shielding against high energy radiotherapy linear accelerator machines (linac) radiation requires deep knowledge about radiation and materials interaction shielding physics and calculations and characteristics of the materials shielding properties against radiation. National Council on Radiation Protection and Measurements (NCRP) report No.144 has recommended some materials for application against high-energy radiation shielding materials in the report [1, 2]. The recommended materials included some concretes with different compositions and element mass density as follows. Ordinary concrete (2.35 g/cm³ density), Magnetite concrete (3.53 g/cm³ density), Barytes concrete (3.35 g/cm³ density), Magnetite and Steel concrete (4.64 g/cm³ density), Limonite and Steel concrete (4.54 g/cm³ density), and Serpentine concrete (2.10 g/cm³ density) were the concrete types recommended by NCRP 144 with the concretes composition elements percentage [1]. Recently, nanoparticles-added concretes or nanoconcretes have been developed for dose reduction in the radiation facilities such as linac houses. The issue was the subject of different researchers' studies and enormous publications can be found in the literature [3-22]. Khosravi *et al.* [16-17] studies approved nanoparticle effect on the materials radiation absorption factors increase. They studied the impact of nano-sized gold particles on the target dose enhancement based on photon beams using by Monte Carlo (MC) method and target dose enhancement factor alterations related to the interaction between the photon beam energy and gold nanoparticles' size in external radiotherapy: using the MC method. Nikbin *et al.* [23] investigated five different concrete mixtures made using magnetite aggregated with 0, 2, 4, 6, and 8% of titanium oxide (TiO₂) nanoparticles. In the study, the examined specimens attenuation coefficients were determined for 662 keV, 1173 keV, and 1332 keV energies of γ -ray of ¹³⁷Cs and ⁶⁰Co radioisotopes emitted radiation. They reported a significant improvement in the radiation shielding properties within specimens, including 8% of TiO₂ nanoparticles. Additionally, from the research obtained results, their main conclusion was that the specimen containing 8% of TiO₂ nanoparticle has the highest radiation shielding characteristics and the linear attenuation coefficient increased by 9, 5, and 4.9% for the γ - ray energies of 1332 keV, 1170 keV, and 662 keV, respectively. Mesbahi and Ghiasi [19] studied the effect of nanoparticles and microparticles, including ordinary

concrete in the shielding properties of the pure concrete and compared PbO₂, Fe₂O₃, WO₃, and, H₄B nanoparticles and microparticles performance in the radiation protection and improvement of the concrete shielding properties. They reported that in the study, it was found that the concrete doped with nano-sized particles showed a higher $\Sigma R/\rho$ (7%) and photon attenuation coefficient (μ/ρ) as (8%) relative to the micro-scale particles cross-section. According to the obtained results, they recommended the application of nano-scale materials in the composition of new concretes (nanoconcretes) for the development of dual protection against photon and neutron radiation. Composition of ordinary concrete in terms of percent of an element in total mass comprised of H (0.005), Si (0.313), Ca (0.0825), Na (0.170), O (0.1902), Al (0.0355), Fe (0.0123), and K (0.191) with the density of 2.35 g/cm³. Various types of nanomaterials were used in addition to the shielding material composition and concrete to modify the radiation shielding properties such as nano-silica, nano-Al₂O₃, tetra ZnO whiskers (T-ZnO), nano-ZnO, nanoparticles of ZrO₂, Cr₂O₃, CuO, CaCO₃, nano-TiO₂, Cu nanomaterial, graphene, Carbon nanotubes, Carbon nanofibers, nano-Boron nitride, and different nano-sized particles or chemical compounds. It was reported that these nanomaterials produce additional C-S-H and provide good shielding materials against radiation [24-26]. Mansouri *et al.* reviewed the neutron shielding performance of nanocomposite materials in radiotherapy energy ranges and showed the good performance of nanomaterials presence in the shielding materials in dose reduction in the radiation field [27]. They estimated neutron shielding properties and moderation using nanostructures and they concluded that the moderator materials in the form of ultra-dispersed particles could be effective for shielding neutrons with lower energies (0.0-0.025 eV) [28]. Kim *et al.* [29], investigated radiation shielding properties enhancement by the use of micro-scale of B₂O₃ with sizes of 200-300 μ m and 0.1-1 μ m (micro-scales sizes) to Polyvinylalcohol (PVA). The study revealed that the macroscopic thermal neutron absorption cross-section was 12% and 13.3% higher than larger particles for the weight concentration of 1% and 2.5%, respectively. Different studies on the effect of nanoparticle size, concentration, chemical composition, and other characteristics were also conducted on the shielding characteristics of the nanoparticle, including concrete or nanoconcrete [30]. Sikora *et al.* [31] compared the effects of microparticles and nanoparticles of Bi₂O₃ powders and reported that the addition of both

microparticles and nanoparticles of the Bi_2O_3 powders enhances the γ -ray shielding capability of the specimen and their main conclusion was a high enhancement of the concrete shielding properties compared to the microparticle included concrete. There are different investigations on the shielding materials' properties enhancement against radiation using MC simulation, experimental and analytical methods, and different nanoparticles' effects on the concrete shielding enhancement employed [31-34]. In the current study, shielding properties enhancement characterization of Fe_2O_3 (5%), WO_3 (5%), B_4H (5%), Pb_2O_3 (5%) 50nm nanoparticles loaded ordinary concrete (nanoconcrete aggregated with the mixture of fore different nanoparticles) were investigated. Additionally, dose reduction due to nanoparticle application in the concrete composition calculated for the secondary produced photoneutron and capture γ -ray besides additional bendings in the maze effect in dose reduction at the maze door location for designing a room with a light door with minimum shielding materials was studied. MCNP5 MC simulation code and N-XCOM computational shielding program were utilized.

2. Materials and Methods

MCNP5/1.60 [35] of the MC simulation code was employed to perform all simulations and calculations in the current study. The physical and geometrical simulation of the problem were conducted in this study using the MC simulation code. MCNP5/1.60 is an enhanced and benchmarked MCNP MC simulation code that was released by the Los-Alamos National Laboratory (LANL), including updated physics data of the complicated phenomena cross-sections. The used MCNP5/1.60 MC simulation code is capable of simulation complex three-dimensional (3D) geometries and physical phenomena. The used MC code can transport a different number of physical and nuclear particles in a wide range of energies through different materials by calculating microscopic interactions between the radiation and materials with a negligible statistical error. It includes rich physics data libraries such as cross-sections and is a flexible and powerful tool that is capable of complex geometrical simulation and complicated three-dimensional (3D) radiation physics problem solving [36]. MC simulation is widely used in the radiation protection physics calculations in the literature [37, 38]. N-XCOM computational program is also employed to determine shielding materials and their composing elements, neutron and photon attenuation

factors. The attenuation factor of the shielding materials and composing elements was estimated using the MC and N-XCOM computational programs. Employment of MCNP5 MC code capabilities, lattice configuration were simulated and filled with concretes with the nanospheres in the created voxels center in 50 nm in diameter. The voxels sides were simulated in 1 μm and filled with the studied concretes. In addition, the main parts of an 18 MV Varian 2100 Clinac were simulated by the employment of the MCNP5/1.60 MC simulation code. Gaussian distributed primary electrons symmetric along with X and Y axes and the Full Width at Half Maximum (FWHM) of 0.087, thin target, bending magnet, target supporter and electron stopper piece and target supporter, primary and secondary collimators and movable jaws, Flattening-Filter (FF) with complex geometry, mirror and ionization chamber and additionally, massive and complex geometry of the linac head shielding were the simulated main parts of the linac head. On the other hand, a $30 \times 30 \times 30 \text{ cm}^3$ water field phantom was positioned at 100 cm Surface-to-Source Distance (SSD) from the linac X-ray source (target). Treatment room of the simulated linac was modeled so that the primary barriers at the maze door were filled with some nanoparticles mixture and photoneutron and capture γ -ray DE calculations were conducted in the radiotherapy room made of nanoparticle-filled nanoconcrete utilizing MC simulation. 10^{11} primary electrons were run for the calculations in our work. Applied nanoparticles of Fe_2O_3 (5%), WO_3 (5%), B_4H (5%), Pb_2O_3 (5%) size was simulated as 50nm, and for each nanoconcrete (Ordinary concrete including nanoparticles mixture) the secondary produced photoneutron and capture γ -ray DE from the linac were calculated at the maze entrance. The room's primary barrier was made of ordinary concrete with a density of 2.35 gr/cm^3 and the secondary produced photoneutron and capture γ -ray DE calculation for the pure concrete-made primary barrier were also estimated. MC simulation method and N-XCOM computational software were used to determine the capture γ -ray and neutron DE at the maze entrance of an 18 MV linac treatment room. Figures 1a and 1b show the maze layout and the room walls filled by the nanoparticles, additional bending as well as dimensions and the MC set up "good geometry" for the neutron and capture γ -ray attenuation factors. A surface positioned around the linac and any produced secondary neutron crossing-on the surface scored by application of F1 tally of the used MCNP5MC code and photon energy deposited was derived by *F8 tally at a cylindrical cell with the mass

of 0.625 gr at isocenter in the water phantom and value of MeV/gr or dose was calculated by absorber mass and deposited energy to the mass of the absorber. The result was converted to Gy (J/Kg) and the primary electrons required to deliver one Gy photon dose to the isocenter were calculated. Then, the produced number of the linac head produced neutrons scored by F1 tally per X-ray Gy absorbed at isocenter ($n_0/X\text{-ray Gy}$) was calculated. The calculated value has been defined by International Atomic Energy Agency (IAEA) safety report no. 47 [2] as apparent neutron source strength (QN) and is necessary for converting the calculation of the neutron dose to Sv/X-ray at the isocenter. The calculated QN is essential in the megavoltage linacs shielding calculations. In Figure 1, the lengths of the first, second, and third legs of the maze were shown as 7 m, 2 m, and 3 m.

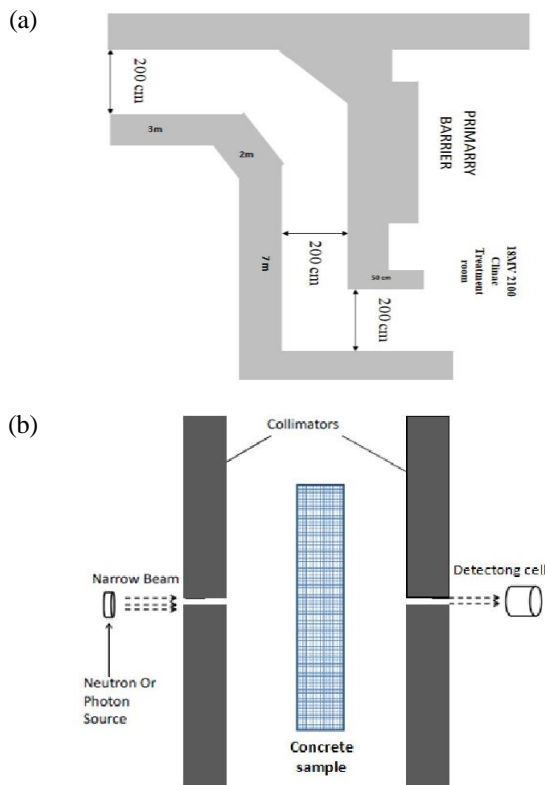


Figure 1. a) A schematic view of the primary barrier made of nano-concrete and additional bend in the maze for designing open-door radiotherapy facility. The Additional bending in the maze and some nano-particles loaded on the primary barrier are the parameters that reduce radiation at the maze entrance to a level that not a door requires to decrease radiation dose to acceptable level, **b)** MC simulation of a good geometry, including collimators, absorber slab (in thickness of 1cm), narrow beam and detecting cell at a distant so that scattered radiations not be scored. Distance of narrow beam to the concrete slab (or other absorber materials) set as 40cm and the slab to the radiation detecting cell set as 60cm

2.1. Effective Neutron Removal Cross-Section

There is a theoretical explanation for the radiation attenuation by the materials such as ΣR in the literature. Neutron removal of a shielding material mainly occurs in Hydrogen rich materials or in the high collisions of the neutron beam and materials. The neutron removal cross-section concept is based on the presence of hydrogen in the absorber. It can also be applied to other hydrogen-rich absorbers. When no hydrogenous materials are present, the neutron removal coefficient ΣR is given by the following Equation.

$$\sum_R (cm^{-1}) = \frac{0.602\rho\delta_t}{A} \quad (1)$$

Where δ_t is the total cross-section in (barns) for each atom in a material in a unit of volume of the absorber material that depends on the neutron energy, ρ is the density (g/cm^3) and A is the atomic mass. $\Sigma R/\rho$ or mass removal coefficients dependent only on the microscopic nuclear properties and smoothly varies with the atomic weight. It has proposed [39] an empirical method to calculate neutron mass removal cross-section as follows (Equation 2).

$$\sum_R / \rho = 0.206A^{-\frac{1}{3}} Z^{-0.294} \left(\frac{cm^2}{g} \right) \quad (2)$$

For more descriptions, the readers can refer to the literature. For the shielding materials that are composed of different nanoparticles or chemical compounds, the following given empirical was recommended to calculate $\Sigma R/\rho$ (Equation 3).

$$\frac{\Sigma R}{\rho} = \sum w_i \left(\frac{\Sigma R}{\rho} \right)_i \quad (3)$$

The readers can refer to the literature for more information [39-44].

3. Results and Discussion

MC calculations were conducted in this study by setting up “good geometry” due to the prevention of scattered radiation reaching and to not scoring the scattered radiation in the detector cell in the simulation in “good geometry”. The room maze geometry and good geometry setup were shown in Figure 1. The neutron attenuation factor calculations for the nanoconcrete, including 20% nanoparticles mixture was conducted using the MC

simulation method and N-XCOM computational shielding software. $\Sigma R/\rho$ in cm^2/g of the nanoparticle-included nanoconcrete and composing elements were derived by MC simulation method and N-XCOM software calculation and the results were tabulated in Tables 1a and 1b. The calculations were conducted for the mono-energetic neutron energy of 1.5 MeV which is the average energy of the photoneutron energy from the medical linear accelerators (linac) [1]. Total $\Sigma R/\rho$ of the neutron with energies of 100 keV-2000 keV was estimated as 0.02802-0.02687 cm^2/g in the MC simulation method in good geometry while N-XCOM software calculated the same values as 0.02810-0.02687 cm^2/g . Additionally, the concrete composition elements $\Sigma R/\rho$ were estimated by MC simulation and XCOM software for the used concrete types that were used in our study. Good agreements were seen between the MC simulation results

and N-XCOM software calculations both for elements and total nanoconcretes $\Sigma R/\rho$ for all types of the nanoconcretes studied in this investigation. Increasing the neutron energy, $\Sigma R/\rho$ decreased slightly and the trend is in agreement with our previous publication [19]. In our previous work, the higher ratio of nanoparticles included concrete/Pure ordinary concrete while the nanoconcretes were doped with the PbO_2 , Fe_2O_3 , WO_3 , and, H_4B on the $2.35 \text{ g}/\text{cm}^3$ ordinary concrete obtained as 14.1 at 100 keV, 14.2 at 100 keV, 14.2 at 100 keV, and 14.2 at 100 keV neutron beam. Our calculations showed the nanoparticle included concrete/Pure ordinary concrete in 100 keV narrow neutron beam as 16.87% which revealed that the presence of 20% of nanoparticles mixture in ordinary concrete composition increased the neutron $\Sigma R/\rho$ more than one nanoparticle loaded concrete. The results are in agreement with Khosravi *et al.* [16-17] works.

Table 1a. Neutron effective mass removal cross-section estimated by MC simulation for the concrete elements and total nanoparticle-included concrete the neutron ($\Sigma R/\rho$ (cm^2/g))

| Energy | H | O | K | Ca | Na | Si | Al | Total Ordinary concrete |
|----------|----------|----------|----------|----------|----------|----------|----------|-------------------------|
| 100 keV | 0.03536 | 0.02486 | 0.03575 | 0.02851 | 0.02714 | 0.03457 | 0.03616 | 0.02802 |
| 200 keV | 0.035219 | 0.024777 | 0.035591 | 0.028402 | 0.027041 | 0.03442 | 0.035999 | 0.02798 |
| 300 keV | 0.035079 | 0.024695 | 0.035434 | 0.028294 | 0.026943 | 0.03427 | 0.035838 | 0.02795 |
| 400 keV | 0.034939 | 0.024613 | 0.035278 | 0.028188 | 0.026846 | 0.034122 | 0.035679 | 0.02791 |
| 500 keV | 0.0348 | 0.024532 | 0.035123 | 0.028082 | 0.026749 | 0.033975 | 0.035521 | 0.02788 |
| 600 keV | 0.034661 | 0.024452 | 0.034968 | 0.027977 | 0.026654 | 0.033829 | 0.035364 | 0.02784 |
| 700 keV | 0.034523 | 0.024372 | 0.034815 | 0.027872 | 0.026558 | 0.033684 | 0.035209 | 0.02780 |
| 800 keV | 0.034386 | 0.024292 | 0.034663 | 0.027768 | 0.026464 | 0.03354 | 0.035054 | 0.02736 |
| 900 keV | 0.034249 | 0.024213 | 0.034512 | 0.027665 | 0.02637 | 0.033396 | 0.0349 | 0.02734 |
| 1000 keV | 0.034112 | 0.024135 | 0.034362 | 0.027563 | 0.026276 | 0.033254 | 0.034747 | 0.02730 |
| 1100 keV | 0.033976 | 0.024057 | 0.034214 | 0.027461 | 0.026184 | 0.033113 | 0.034596 | 0.02724 |
| 1200 keV | 0.033841 | 0.02398 | 0.034066 | 0.027361 | 0.026092 | 0.032973 | 0.034445 | 0.02720 |
| 1300 keV | 0.033706 | 0.023903 | 0.033919 | 0.02726 | 0.026 | 0.032834 | 0.034296 | 0.02718 |
| 1400 keV | 0.033572 | 0.023827 | 0.033773 | 0.027161 | 0.02591 | 0.032695 | 0.034148 | 0.02713 |
| 1500 keV | 0.033438 | 0.023752 | 0.033628 | 0.027062 | 0.025819 | 0.032558 | 0.034 | 0.02710 |
| 1600 keV | 0.033305 | 0.023677 | 0.033485 | 0.026964 | 0.02573 | 0.032422 | 0.033854 | 0.02707 |
| 1700 keV | 0.033172 | 0.023602 | 0.033342 | 0.026866 | 0.025641 | 0.032286 | 0.033709 | 0.02701 |
| 1800 keV | 0.03304 | 0.023528 | 0.0332 | 0.02677 | 0.025553 | 0.032152 | 0.033564 | 0.02802 |
| 1900 keV | 0.032908 | 0.023454 | 0.033059 | 0.026674 | 0.025465 | 0.032019 | 0.033421 | 0.02696 |
| 2000 keV | 0.032777 | 0.023381 | 0.03292 | 0.026578 | 0.025378 | 0.031886 | 0.033279 | 0.02687 |

Table 1b. Neutron effective mass removal cross-section calculated by N-XCOM for the neutron for concrete elements and total nanoparticle-included concrete

| Energy | H | O | K | Ca | Na | Si | Al | Total nano-concrete |
|----------|----------|----------|----------|----------|----------|----------|----------|---------------------|
| 100 keV | 0.024897 | 0.035841 | 0.028565 | 0.027188 | 0.034655 | 0.036253 | 0.024897 | 0.02810 |
| 200 keV | 0.024813 | 0.035682 | 0.028456 | 0.027089 | 0.034504 | 0.036091 | 0.024813 | 0.02801 |
| 300 keV | 0.024731 | 0.035524 | 0.028348 | 0.02699 | 0.034354 | 0.03593 | 0.024731 | 0.02798 |
| 400 keV | 0.024649 | 0.035367 | 0.028241 | 0.026893 | 0.034205 | 0.03577 | 0.024649 | 0.02790 |
| 500 keV | 0.024567 | 0.035211 | 0.028135 | 0.026796 | 0.034057 | 0.035611 | 0.024567 | 0.02785 |
| 600 keV | 0.024486 | 0.035056 | 0.028029 | 0.026699 | 0.03391 | 0.035454 | 0.024486 | 0.02780 |
| 700 keV | 0.024406 | 0.034902 | 0.027924 | 0.026603 | 0.033764 | 0.035297 | 0.024406 | 0.02777 |
| 800 keV | 0.024326 | 0.034749 | 0.02782 | 0.026508 | 0.03362 | 0.035141 | 0.024326 | 0.02772 |
| 900 keV | 0.024247 | 0.034597 | 0.027716 | 0.026414 | 0.033476 | 0.034987 | 0.024247 | 0.02743 |
| 1000 keV | 0.024168 | 0.034447 | 0.027613 | 0.02632 | 0.033333 | 0.034834 | 0.024168 | 0.02735 |
| 1100 keV | 0.02409 | 0.034297 | 0.027511 | 0.026227 | 0.033191 | 0.034681 | 0.02409 | 0.02724 |
| 1200 keV | 0.024012 | 0.034148 | 0.02741 | 0.026135 | 0.03305 | 0.03453 | 0.024012 | 0.02720 |
| 1300 keV | 0.023935 | 0.034001 | 0.027309 | 0.026043 | 0.03291 | 0.03438 | 0.023935 | 0.02718 |
| 1400 keV | 0.023859 | 0.033854 | 0.027209 | 0.025952 | 0.032771 | 0.034231 | 0.023859 | 0.02713 |
| 1500 keV | 0.023783 | 0.033709 | 0.02711 | 0.025861 | 0.032633 | 0.034083 | 0.023783 | 0.02710 |
| 1600 keV | 0.023707 | 0.033564 | 0.027011 | 0.025771 | 0.032496 | 0.033936 | 0.023707 | 0.02707 |
| 1700 keV | 0.023632 | 0.033421 | 0.026913 | 0.025682 | 0.03236 | 0.03379 | 0.023632 | 0.02701 |
| 1800 keV | 0.023558 | 0.033278 | 0.026816 | 0.025593 | 0.032225 | 0.033644 | 0.023558 | 0.02802 |
| 1900 keV | 0.023484 | 0.033137 | 0.026719 | 0.025505 | 0.032091 | 0.0335 | 0.023484 | 0.02696 |
| 2000 keV | 0.023411 | 0.032996 | 0.026623 | 0.025418 | 0.031958 | 0.033357 | 0.023411 | 0.02687 |

Our results were in good agreement with the published works in the literature [19, 31, 45]. Tekin *et al.* studied the size of the particles loaded on the concrete effect on the shielding enhancement and concluded that the size of the WO_3 affected the mass attenuation coefficients of concrete in all photon energies [45]. Ghasemi and Ghiasi [10] designed a linac treatment room with primary barriers doped with a mixture of some nanoparticles (each with 1.5% wt) and it reduced effectively the walls shielding characteristics. Our results showed more dose reduction due to more nanoparticles presence in the ordinary concrete composition. In Figures 1a and 1b, the maze layout and good geometry for data deriving avoiding scattered radiation were shown. Additionally, in Figures 2a to 2g photon neutron at different points of the maze and the effect of each studied nanoparticle besides the total

neutron compared to the walls with nanoparticles mixture studied. Capture γ -ray fluence and effect of each mixture nanoparticle was estimated for the Secondary neutron and capture γ -ray dose equivalent at the maze entrance. In the current study, the nanoparticle-loaded ordinary concrete made 18 MV Varian 2100 Clinic bunker maze entrance neutron and captured γ -ray DE were estimated. Photon dose equivalent (Sv/e) at the isocentre was estimated as 0.12×10^{-15} primary electrons. According to the estimations, it was predicted that 8.33×10^{14} primary electrons are required to run to deliver 1 X-ray Gy DE to the isocentre to simulate incidence on the thick target of the linac. With the obtained number of primary electrons running, 1.34×10^{12} neutrons were produced per isocenter X-ray Gy or QN. Then the simulated linac QN obtained as 1.34×10^{12} n/Gy which was in good agreement with the literature.

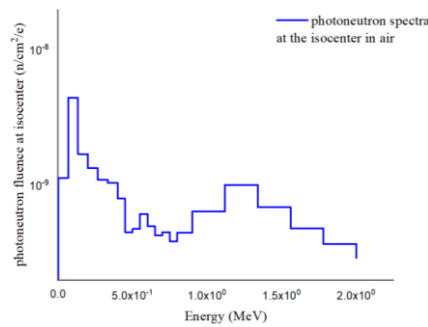


Figure 2a. Photoneutron spectra at the isocentre from the simulate 18MV Varian 2100 Clinac derived by MCNP5 MC simulation code in the water phantom

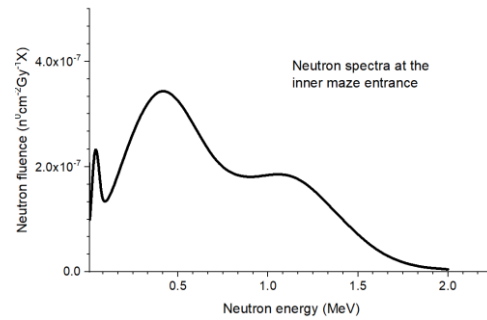


Figure 2b. Photoneutron fluence at the inner maze entrance from the modeled 18MV Varian 2100 Clinac derived by MCNP5 MC Simulation code

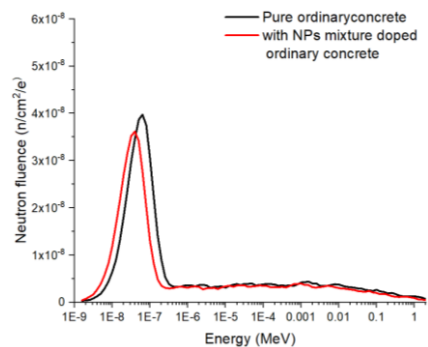


Figure 2c. Photoneutron spectra from the modeled 18MV Varian 2100Clinacat the middle of maze behind the primary barrier with pure ordinary concrete and nanoparticles mixture doped ordinary concrete

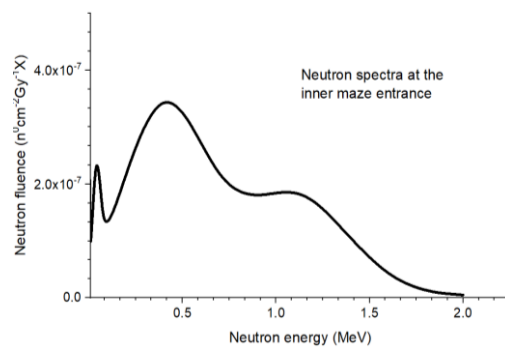


Figure 2d. Photoneutron fluence at the inner maze entrance from the modeled 18MV Varian 2100 Clinac derived by MCNP5 MC Simulation code

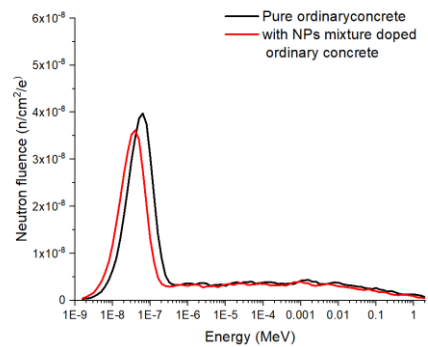


Figure 2e. Photoneutron spectra from the modeled 18MV Varian 2100Clinacat the middle of maze behind the primary barrier with pure ordinary concrete and nanoparticles mixture doped ordinary concrete

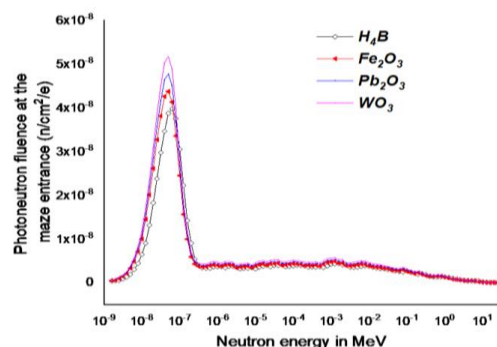


Figure 2f. Photoneutron spectra at the maze entrance and effect of nanoparticles in the mixture doped on the concrete. According to the spectra, B4H nanoparticle affected Photon neutron fluence more than other nanoparticle affected

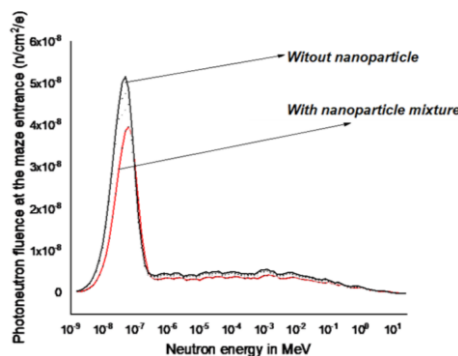


Figure 2g. Photoneutron fluence at the maze entrance of the room made of ordinary concrete with and without nanoparticles mixture

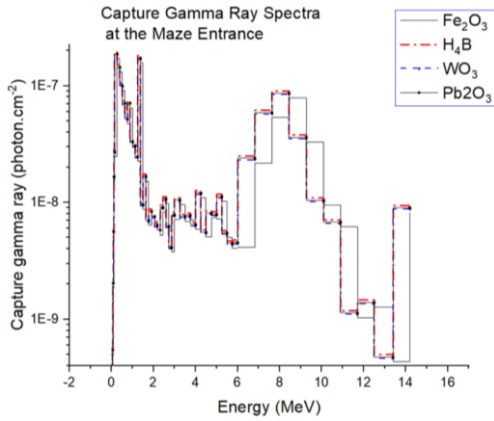


Figure 3a. Capture γ ray at the maze entrance and effect of each nanoparticle on the fluence

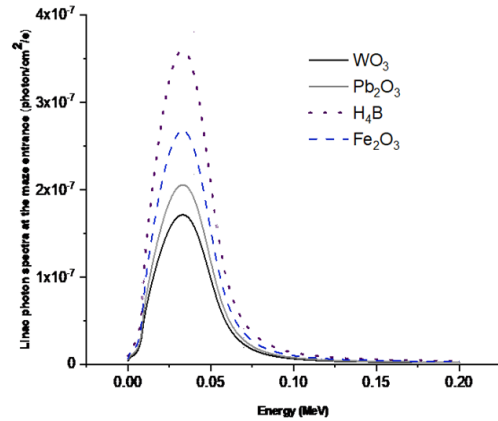


Figure 3b. Scattered photon from the linac head, transmission from the maze wall and maze that total photon fluence at the maze entrance was derived by MC simulation, H4B for higher hydrogen captured more neutrons and emitted more capture γ -ray

In the simulated room maze layout and dimension which was shown in Figure 1a, neutron and capture γ -ray dose equivalent estimated by MC simulation method. The simulated maze includes 3 bendings and there is no recommended empirical method for the neutron and capture γ -ray dose equivalent calculation at the maze entrance of the 18 MV linac room. MCNP5/1.60 MC simulation code was calculated secondary neutron and capture γ -ray dose equivalent to 1.65×10^{07} mSv/isocenter Gy and 7.98×10^{-06} mSv/isocenter Gy (Figure 3a & 3b). Ghasemi and Ghiasi [10, 46] derived neutron at the maze entrance of a room with the primary barriers, including nanoparticles mixture as 1.56×10^{-03} Gy and 9.65×10^{-05} mSv/isocenter Gy at 50 cm inner of the door and 50cm outer of the door. We calculated the neutron dose equivalent at the door location and for the open-door maze. The lower DE estimated in our work can be attributed to the nanoparticles in concrete composition and additional bendings in the maze layouts which affect the neutron interaction with the maze walls and decreases the neutron energy as two main effects. The calculated neutron DE at a straight maze may be the origin of the observed differences. As the maze entrance and door are located in the controlled area, and the recommended design limits the controlled area and the fact that the recommended dose limit for the control area is 0.1 mSv/week [2], the required number of shielding materials Tenth Value Layer (TVL) was recommended to calculate with (Equation 4):

$$\text{No. of TVL} = \log_{10} \frac{DE(\text{mSv per week})}{0.1(\text{mSv per week})} \quad (4)$$

Then, according to Equation 4, TVL number of neutron shielding material in the maze door (Borated-Polyethylene) or BPE, obtained as 1.65×10^{-04} . Using one TVL of 45 mm for BPE derived from the IAEA no.47 report, the required thickness was derived as 7.43×10^{-06} mm for the neutron shielding. 4.73×10^{-06} mm lead was also required for the capture γ -ray shielding. The results are close to Open-Door megavoltage 18MV linac-based radiotherapy.

4. Conclusion

We concluded that additional bending in the room maze and the presence of some nanoparticles mixture in the bunker concrete performed as two effective factors in the reduction of the radiation contamination at the maze entrance. Lightening or removing the maze door is important in the patient treatment in the patients psychologically and also getting rid of the door interlock. We predict that by increasing some nanoparticles or increasing the primary barrier thickness, it may be possible to design an Open-Door small mazes megavoltage linac radiotherapy room. Further studies are strongly proposed by the authors to design an Open-Door megavoltage radiotherapy room for patient psychology help and personnel technical convenience.

References

- 1- Francesco d'Errico, "NCRP Report no. 144—Radiation protection for particle accelerator facilities National Council on Radiation Protection and Measurements Issued 31 December 2003.

- 2- International Atomic Energy Agency, Radiation protection in the design of radiotherapy facilities. *Internat. Atomic Energy Agency*, (2006).
- 3- Jamal A Abdalla, Blessen Skariah Thomas, Rami A Hawileh, Jian Yang, Bharat Bhushan Jindal, and Erandi Ariyachandra, "Influence of nano-TiO₂, nano-Fe₂O₃, nanoclay and nano-CaCO₃ on the properties of cement/geopolymer concrete." *Cleaner Materials*, p. 100061, (2022).
- 4- Yas Al-Hadeethi, MI Sayyed, Abeer Z Barasheed, Moustafa Ahmed, and M Elsafi, "Preparation and radiation attenuation properties of ceramic ball clay enhanced with micro and nano ZnO particles." *Journal of Materials Research and Technology*, Vol. 17pp. 223-33, (2022).
- 5- DA Alonso-De la Garza, AM Guzmán, C Gómez-Rodríguez, DI Martínez, and N Elizondo, "Influence of Al₂O₃ and SiO₂ nanoparticles addition on the microstructure and mechano-physical properties of ceramic tiles." *Ceramics International*, Vol. 48 (No. 9), pp. 12712-20, (2022).
- 6- F Amor, M Baudys, Z Racova, L Scheinherrová, L Ingrisova, and P Hajek, "Contribution of TiO₂ and ZnO nanoparticles to the hydration of Portland cement and photocatalytic properties of High Performance Concrete." *Case Studies in Construction Materials*, Vol. 16p. e00965, (2022).
- 7- Soudabeh Dezhmpanah, Iman M Nikbin, Sadegh Mehdipour, Reza Mohebbi, and HamidHabibi Moghadam, "Fiber-reinforced concrete containing nano-TiO₂ as a new gamma-ray radiation shielding materials." *Journal of Building Engineering*, Vol. 44p. 102542, (2021).
- 8- M Elsafi, MA El-Nahal, MI Sayyed, IH Saleh, and MI Abbas, "Effect of bulk and nanoparticle Bi₂O₃ on attenuation capability of radiation shielding glass." *Ceramics International*, Vol. 47 (No. 14), pp. 19651-58, (2021).
- 9- M Elsafi, MI Sayyed, Aljawhara H Almuqrin, MM Gouda, and AM El-Khatib, "Analysis of particle size on mass dependent attenuation capability of bulk and nanoparticle PbO radiation shields." *Results in Physics*, Vol. 26p. 104458, (2021).
- 10- Amir Ghasemi-Jangjoo and Hosein Ghiasi, "MC safe bunker designing for an 18MV linac with nanoparticles included primary barriers and effect of the nanoparticles on the shielding aspects." *Reports of Practical Oncology and Radiotherapy*, Vol. 24 (No. 4), pp. 363-68, (2019).
- 11- Nazanin Gholami, Bahram Ghasemi, Bagher Anvaripour, and Sahand Jorfi, "Enhanced photocatalytic degradation of furfural and a real wastewater using UVC/TiO₂ nanoparticles immobilized on white concrete in a fixed-bed reactor." *Journal of industrial and engineering chemistry*, Vol. 62pp. 291-301, (2018).
- 12- VM Hatkar, VJ Patil, YE Bhoge, JS Narkhede, UD Patil, and RD Kulkarni, "Solution spray synthesis and surface modification of SiO₂ nanoparticle for development of UV curable concrete coatings." *Vacuum*, Vol. 147pp. 158-62, (2018).
- 13- Amal Fadhil Kamil, Hussain Ismail Abdullah, Ahmed Mahdi Rheima, and Srwa Hashim Mohammed, "UV-Irradiation synthesized α -Fe₂O₃ nanoparticles based dye-sensitized solar cells." *Materials Today: Proceedings*, Vol. 61pp. 820-25, (2022).
- 14- Mahdih Keramati and Bitu Ayati, "Petroleum wastewater treatment using a combination of electrocoagulation and photocatalytic process with immobilized ZnO nanoparticles on concrete surface." *Process Safety and Environmental Protection*, Vol. 126pp. 356-65, (2019).
- 15- S Khannyra, MJ Mosquera, Mohammed Addou, and MLA Gil, "Cu-TiO₂/SiO₂ photocatalysts for concrete-based building materials: Self-cleaning and air de-pollution performance." *Construction and Building Materials*, Vol. 313p. 125419, (2021).
- 16- Hossein Khosravi, Bijan Hashemi, Seyed Rabie Mahdavi, and Payman Hejazi, "Target dose enhancement factor alterations related to interaction between the photon beam energy and gold nanoparticles' size in external radiotherapy: using Monte Carlo method." *Koomesh*, pp. 255-61, (2015).
- 17- Hossein Khosravi, Armita Mahdavi, Faezeh Rahmani, and Ahmad Ebadi, "The impact of nano-sized gold particles on the target dose enhancement based on photon beams using by Monte Carlo Method." *Nanomedicine Research Journal*, Vol. 1 (No. 2), pp. 84-89, (2016).
- 18- Mohamed E Mahmoud, Rehab M El-Sharkawy, Elhassan A Allam, Reda Elsaman, and Atef El-Taher, "Fabrication and characterization of phosphotungstic acid-Copper oxide nanoparticles-Plastic waste nanocomposites for enhanced radiation-shielding." *Journal of Alloys and Compounds*, Vol. 803pp. 768-77, (2019).
- 19- Asghar Mesbahi and Hosein Ghiasi, "Shielding properties of the ordinary concrete loaded with micro-and nanoparticles against neutron and gamma radiations." *Applied Radiation and Isotopes*, Vol. 136pp. 27-31, (2018).
- 20- Rosangel Ortega-Villar, Liliana Lizárraga-Mendiola, Claudia Coronel-Olivares, Luis D López-León, Carlos Alfredo Bigurra-Alzati, and Gabriela A Vázquez-Rodríguez, "Effect of photocatalytic Fe₂O₃ nanoparticles on urban runoff pollutant removal by permeable concrete." *Journal of environmental management*, Vol. 242pp. 487-95, (2019).
- 21- HO Tekin, MI Sayyed, and Shams AM Issa, "Gamma radiation shielding properties of the hematite-serpentine concrete blended with WO₃ and Bi₂O₃ micro and nano particles using MCNPX code." *Radiation Physics and Chemistry*, Vol. 150pp. 95-100, (2018).
- 22- C Thomas, J Rico, P Tamayo, J Setién, F Ballester, and JA Polanco, "Neutron shielding concrete incorporating B₄C and PVA fibers exposed to high temperatures." *Journal of Building Engineering*, Vol. 26p. 100859, (2019).
- 23- Iman M Nikbin, Mojtaba Shad, Gholam Ali Jafarzadeh, and Soudabeh Dezhmpanah, "An experimental investigation on combined effects of nano-WO₃ and nano-Bi₂O₃ on the

- radiation shielding properties of magnetite concretes." *Progress in Nuclear Energy*, Vol. 117p. 103103, (2019).
- 24- Tuan Anh Nguyen, Thi Lua Pham, Thi Mai Thanh Dinh, Hoang Thai, and Xianming Shi, "Application of nano-SiO₂ and nano-Fe₂O₃ for protection of steel rebar in chloride contaminated concrete: epoxy nanocomposite coatings and nano-modified mortars." *Journal of nanoscience and nanotechnology*, Vol. 17 (No. 1), pp. 427-36, (2017).
- 25- NB Singh, "Properties of cement and concrete in presence of nanomaterials." in *Smart Nanoconcretes and Cement-Based Materials: Elsevier*, (2020), pp. 9-39.
- 26- NB Singh, Meenu Kalra, and SK Saxena, "Nanoscience of cement and concrete." *Materials Today: Proceedings*, Vol. 4 (No. 4), pp. 5478-87, (2017).
- 27- E Mansouri, A Mesbahi, R Malekzadeh, A Ghasemi Janghjo, and MURAT Okutan, "A review on neutron shielding performance of nanocomposite materials." *International Journal of Radiation Research*, Vol. 18 (No. 4), pp. 611-22, (2020).
- 28- VA Artem'Ev, "Estimate of neutron attenuation and moderation by nanostructural materials." *Atomic Energy*, Vol. 94 (No. 4), pp. 282-85, (2003).
- 29- Jaewoo Kim, Young Rang Uhm, Min-Ku Lee, Hee Min Lee, and Chang Kyu Rhee, "Neutron shielding characteristics of nano-B₂O₃ dispersed Poly Vinyl Alcohol." in *Transactions of the Korean Nuclear Society Spring Meeting May*, (2008), Vol. 29, pp. 29-30.
- 30- Ş Gözde İrim *et al.*, "Physical, mechanical and neutron shielding properties of h-BN/Gd₂O₃/HDPE ternary nanocomposites." *Radiation Physics and Chemistry*, Vol. 144pp. 434-43, (2018).
- 31- Pawel Sikora, Ahmed M El-Khayatt, HA Saudi, Sang-Yeop Chung, Dietmar Stephan, and Mohamed Abd Elrahman, "Evaluation of the effects of bismuth oxide (Bi₂O₃) micro and nanoparticles on the mechanical, microstructural and γ -ray/neutron shielding properties of Portland cement pastes." *Construction and Building Materials*, Vol. 284p. 122758, (2021).
- 32- Zhipeng Huo, Sheng Zhao, Guoqiang Zhong, Hong Zhang, and Liquan Hu, "Surface modified-gadolinium/boron/polyethylene composite with high shielding performance for neutron and gamma-ray." *Nuclear Materials and Energy*, Vol. 29p. 101095, (2021).
- 33- Seulgi Kim, Yunhee Ahn, Sung Ho Song, and Dongju Lee, "Tungsten nanoparticle anchoring on boron nitride nanosheet-based polymer nanocomposites for complex radiation shielding." *Composites Science and Technology*, Vol. 221p. 109353, (2022).
- 34- Dong Zhou, Quan-Ping Zhang, Jian Zheng, You Wu, Yang Zhao, and Yuan-Lin Zhou, "Co-shielding of neutron and γ -ray with bismuth borate nanoparticles fabricated via a facile sol-gel method." *Inorganic Chemistry Communications*, Vol. 77pp. 55-58, (2017).
- 35- Monte Carlo Team, "MCNP-A general N-Particle Transport Code, Version 5." *vol. I, Overview and Theory*, (2005).
- 36- Chaocheng Kong *et al.*, "Monte Carlo method for calculating the radiation skyshine produced by electron accelerators." *Nuclear Instruments and Methods in Physics Research Section B: Beam Interactions with Materials and Atoms*, Vol. 234 (No. 3), pp. 269-74, (2005).
- 37- Pedro Andreo, "Monte Carlo techniques in medical radiation physics." *Physics in Medicine & Biology*, Vol. 36 (No. 7), p. 861, (1991).
- 38- Joao Seco and Frank Verhaegen, Monte Carlo techniques in radiation therapy. *CRC press Boca Raton, FL:*, (2013).
- 39- Maurice F Kaplan, "Concrete radiation shielding." (1989).
- 40- Arthur B Chilton, J Kenneth Shultis, and Richard E Faw, "Principles of radiation shielding." (1984).
- 41- Protection Against Neutron Radiation, "Report No. 38." *National Council on Radiation Protection and Measurements, Bethesda*, (1971).
- 42- Nicholas Tsoulfanidis, "Computational methods in reactor shielding." ed: *Taylor & Francis*, (1984).
- 43- MILLION ELECTRON VOLTS, "Protection Against Neutron Radiation up to 30 Million Electron Volts." (1957).
- 44- ME Wieser, "Atomic weights of the elements 2005 (IUPAC Technical Report)." *Pure and Applied Chemistry*, Vol. 78 (No. 11), pp. 2051-66, (2006).
- 45- Huseyin Ozan Tekin, Viswanath P Singh, and Tugba Manici, "Effects of micro-sized and nano-sized WO₃ on mass attenuation coefficients of concrete by using MCNPX code." *Applied Radiation and Isotopes*, Vol. 121pp. 122-25, (2017).
- 46- Asghar Mesbahi, Hosein Ghiasi, and Rabee Seyed Mahdavi, "Photoneutron and capture gamma dose calculations for a radiotherapy room made of high density concrete." *Nuclear Technology and Radiation Protection*, Vol. 26 (No. 2), pp. 147-52, (2011).